HHS Public Access

Author manuscript

J Immunol. Author manuscript; available in PMC 2016 June 15.

Published in final edited form as:

J Immunol. 2015 June 15; 194(12): 5926–5936. doi:10.4049/jimmunol.1500385.

The frequency of naïve and early-activated hapten-specific B cell subsets dictates the efficacy of a therapeutic vaccine against prescription opioid abuse

Megan Laudenbach[*], **Federico Baruffaldi**[*,†], **Jeffrey S Vervacke**[‡], **Mark D Distefano**[‡], **Philip J Titcombe**[§], **Daniel L Mueller**[§], **Noah J Tubo**[¶], **Thomas S Griffith**[‖], and **Marco Pravetoni**[*,#,**]

[*]Minneapolis Medical Research Foundation, Minneapolis, USA

[†]Universita degli Studi di Milano, Facolta di Scienze Farmacologiche, Milan, Italy

[‡]Department of Chemistry, University of Minnesota, Minneapolis, MN, USA

[§]Department of Medicine, Center for Immunology, University of Minnesota, Minneapolis, MN, USA

[¶]Center for Immunology, Department of Microbiology, University of Minnesota, Minneapolis, MN, USA

[‖]Department of Urology, University of Minnesota, Minneapolis, MN, USA

[#]Department of Medicine, University of Minnesota, Minneapolis, MN, USA

[**]Department of Pharmacology, University of Minnesota, Minneapolis, MN, USA

Abstract

Translation of therapeutic vaccines for addiction, cancer or other chronic non-communicable diseases has been slow because only a small subset of immunized subjects achieved effective antibody levels. We hypothesize that individual variability in the number of naïve and early-activated hapten-specific B cells determines post-vaccination serum antibody levels and vaccine efficacy. Using a model vaccine against the highly abused prescription opioid oxycodone, the polyclonal B cell population specific for an oxycodone-based hapten (6OXY) was analyzed by flow cytometry paired with antigen-based magnetic enrichment. A higher frequency of 6OXY-specific B cells in either spleen biopsies or blood, before and after immunization, correlated to subsequent greater oxycodone-specific serum antibody titers and their efficacy in blocking oxycodone distribution to the brain and oxycodone-induced behavior in mice. The magnitude of 6OXY-specific B cell activation and vaccine efficacy was tightly correlated to the size of the $CD4^+$ T cell population. The frequency of enriched 6OXY-specific B cells was consistent across various mouse tissues. These data provide novel evidence that variations in the frequency of naïve or early-activated vaccine-specific B and T cells can account for individual responses to vaccines and may predict the clinical efficacy of a therapeutic vaccine.

Corresponding author: Marco Pravetoni, prave001@umn.edu, phone 612-232 7017, Minneapolis Medical Research Foundation, 701 Park Avenue South, Minneapolis, 55404 MN.

Current address for Noah J Tubo: Genzyme, a Sanofi company, 49 New York Ave, Framinghman, MA 01701.

The oxycodone vaccine was disclosed in patent US20140093525-A1. Authors have no financial interests.

Introduction

Vaccines have been the most effective medical intervention for infective diseases (1) and have shown promising proof of concept for the treatment of chronic diseases including drug addiction (2; 3), cancer (4) and Alzheimer's disease (5). Yet, therapeutic vaccine efficacy is only met in the subset of immunized animal or human subjects with the highest serum antibody levels against drugs of abuse (6; 7), tumor-associated small carbohydrate and peptide antigens (8; 9), or β amyloid-derived peptides (5). The mechanism(s) underlying individual variability in vaccine efficacy is poorly understood, and it is unclear whether the generation of an effective response, or the lack thereof, is due to vaccine design, disease heterogeneity, host genetics, or interactions between the vaccine and the host immune system.

The development of vaccines against non-communicable diseases has the potential to significantly impact public health (1). For instance, drug addiction is a worldwide concern (10). In the USA, tobacco use is the leading preventable cause of death that is responsible for ∼480,000 deaths annually (11). Similarly, ∼2.1 million people in the USA are addicted to prescription opioid analgesics, and ∼17,000 overdose deaths are attributable to opioid analgesics annually (11). Intravenous drug use is also a known vehicle for blood-borne pathogens, including HIV (11). Despite the high prevalence of opiate abuse, only a few medications exist (12; 13). Also, no treatments are approved for cocaine and methamphetamine dependence, supporting the need for new therapies (14). Vaccines, combined with current medications, may offer a treatment option for drug addiction. Vaccines against drugs of abuse consist of drug-derived haptens bound to foreign immunogenic carriers to stimulate T cell-dependent B cell activation and generate antibodies that bind drugs of abuse in serum, decreasing the distribution of free drug (i.e. unbound) to the brain and addiction-related behaviors.

In germinal centers (GC), antigen-specific GC B cells interact with $CD4^+$ T follicular helper cells (TfH) (15; 16) and mature into either long-lived memory or antibody-secreting B cells (17), which are critical to generate effective antibodies. We hypothesize that the frequency of hapten-specific B cells and carrier-specific $CD4^+$ T cells prior to immunization contributes to vaccine efficacy, as the number of naïve peptide-specific $CD4^+$ T cells can dictate the magnitude of a response to immunization (18). Moreover, $CD4^+$ T cells specific for tetanus toxoid (TT) or keyhole limpet hemocyanin (KLH), proteins commonly used as carriers in conjugate vaccines, are present in different individual frequencies in human blood (19). Similarly, B cells specific for chicken ovalbumin (OVA), phycoerythrin (PE), or other model proteins have different population sizes in the naïve mouse repertoire (20-22). These data suggest that the frequency of T and B cells specific for peptides or proteins may explain some of the variability observed in vaccinated individuals. In contrast, it is not known whether the initial size of the polyclonal hapten-specific B cell subsets shapes the post-vaccination response. Here, we examined the extent to which the number of polyclonal naïve and early-activated hapten-specific B cells correlated to the efficacy of therapeutic vaccines for drug addiction and whether the frequency of hapten-specific B cells in blood provided predictive markers of vaccine clinical efficacy.

To address these central questions in vaccinology, we adopted a state-of-the-art antigen-based enrichment paired with flow cytometry analysis of antigen-specific B cells in the entire B cell repertoire in naïve and immunized mice (20), and applied it to study scarce B cells specific for haptens used in addiction vaccines (23). Here, we tested the extent to which the hapten-specific B cell subsets relate to the efficacy of a conjugate immunogen consisting of an oxycodone-based hapten (6OXY) conjugated to KLH (6OXY-KLH), which showed promising pre-clinical efficacy in blocking oxycodone and hydrocodone distribution to the brain and their behavioral effects (24; 25), including blockage of oxycodone self-administration (26). Our results suggest that the frequency of the naïve and early-activated 6OXY-specific B cells, before and after immunization, correlates with subsequent vaccine efficacy against oxycodone. These findings were supported by the reduction in 6OXY-specific B cells upon selective depletion of $CD4^+$ T cells resulting in loss of vaccine efficacy, and by the observation that increased numbers of carrier-specific $CD4^+$ T cells prior to immunization correlate to greater vaccine efficacy. We discuss the implications of these data with respect to the possibility of identifying patients most likely to benefit from vaccination, and how our findings could aid in the development of therapeutic vaccines against drug addiction or other non-communicable chronic diseases.

Materials and Methods

Study design

A first study analyzed hapten-specific B cells by spleen biopsy before and after immunization in three mouse cohorts (n=24 BALB/c mice). A second study analyzed B cells in blood before and after immunization in an independent cohort of mice (n=24 BALB/c mice). We established *a priori* that within-group linear regression analysis required at least 12 mice for each group, based on previous studies (23; 25). A control study tested whether $CD4^+$ T cells depletion prevented vaccine efficacy (n=6 C57Bl/6 mice), and then, whether the number of carrier-specific $CD4^+$ T helper cells in spleen biopsy prior to immunization correlated with vaccine efficacy (n=9 C57Bl/6 mice). We established *a priori* that T test and one-way ANOVA between groups required at least 6 mice per group. Mouse studies were performed in a treatment-blind fashion.

Ethics statement

Mouse studies conformed to the U.S Department of Health and Human Services Guide for the Care and Use of Laboratory Animals, and the Minneapolis Medical Research Foundation and University of Minnesota Animal Care and Use Committees.

Drugs

Oxycodone was obtained through the NIDA Drug Supply Program and Sigma (St. Louis, MO). Drug doses and concentrations are expressed as the weight of the base.

Synthesis of oxycodone hapten and conjugation to proteins

An oxycodone-based hapten with a tetraglycine linker at the C6 position (6OXY) was synthesized from oxycodone. For ELISA, 6OXY was conjugated to OVA (Sigma, St. Louis, MO). For immunization studies, the 6OXY was conjugated to KLH (Thermo Fisher,

Rockford, IL), and to OVA previously conjugated to the 2W1S peptide (EAWGALANWAVDSA, Genscript) and designated as 6OXY-OVA^{2W}.

Fluorescent reagents for antigen-specific B and T cell analysis

For B cell analysis, the 6OXY hapten was conjugated to PE (Prozyme, Hayward, CA) and designated as $(6OXY)_n$-PE (23). PE was conjugated to the fluorescent dye Alexa Fluor 647 (AF647, Molecular Probes®, Life Technologies, Grand Island, NY), and their conjugation verified by UV spectrometry (23). To increase the B cell analysis sensitivity, the 6OXY, or the tetraglycine linker as control, was conjugated to the N-term of a EAWGALANAWKV peptide containing a biotin-$(PEG)_4$ moiety (b) attached to a C-term lysine (K) amine side chain (below synthesis details). The resulting 6OXY$(Gly)_4$-EAWGALANAW$(K)_b$V and the control peptide NH_2-$(Gly)_4$EAWGALANAW$(K)_b$V conjugates were attached respectively to a streptavidin (SA)-PE conjugate (SA-PE, Prozyme) or a SA-PE labeled with AF674 to provide [6OXY$(Gly)_4$EAWGALANAW$(K)_b$V]$_4$-SA-PE (designated as $(6OXY)_4$-SA-PE) and the decoy reagent [NH_2-$(Gly)_4$EAWGALANAW$(K)_b$V]$_4$-SA-PE-AF647 (designated as (control peptide)$_4$-SA-PE-AF647). The $(6OXY)_4$-SA-PE and the (control peptide)$_4$-SA-PE-AF647 were purified by standard dialysis, and concentrations measured by UV spectrometry. The 2W1S:I-A^b monomers were prepared, biotinylated, and attached to SA conjugated to either PE or APC (27).

Synthesis overview of the 6OXY$(Gly)_4$-EAWGALANAW$(K)_b$V

The 6OXY hapten or the linker alone were conjugated to the N-term of the EAWGALANAWKV peptide containing a biotin-$(PEG)_4$ moiety (b) attached to the C-term lysine (K) side chain. Peptides were prepared by solid phase synthesis using standard Fmoc protection as described (28). For N-term 6OXY hapten conjugation, the N-term Fmoc group was removed and the resulting free amine reacted with the hapten carboxylate using HBTU as the coupling agent followed by global acidic deprotection and resin cleavage (28). For C-terminal side chain biotinylation, a Fmoc-Lys(Dde) residue was incorporated during peptide synthesis. The Dde protecting group was removed using hydrazine, the resulting free amine coupled to a biotin-$(PEG)_4$-N-succinimidyl ester followed by global deprotection, and conjugates purified by reversed-phase HPLC and characterized via NMR and LC-MS.

Detailed synthesis of the 6OXY$(Gly)_4$-EAWGALANAW$(K)_b$V

Peptide synthesis was carried out using an automated solid-phase peptide synthesizer (PS3, Protein Technologies Inc., Memphis, TN) employing standard Fmoc/HCTU based chemistry using amino acid building blocks with typical acid-labile side-chain protecting groups. Synthesis began on preloaded Fmoc-Gly-Wang resin (0.10 mmol) and the peptide chain was elongated using HCTU/N-methylmorpholine-catalyzed, single coupling steps with 4 eq of both protected amino acids and HTCU for 30 min. To facilitate biotinylation at the end of the synthesis, the penultimate lysine residue was installed using Fmoc-Lys(Dde)-OH to provide an orthogonally protected side-chain amine. Following complete chain elongation, the peptide's N-terminus was deprotected with 5% piperidine in DMF (v/v) and the presence of the resulting free amine was confirmed by ninhydrin analysis. The resin containing the peptide was washed with CH_2Cl_2, dried *in vacuo* overnight, weighed, and divided into two

portions for further synthesis on a reduced scale. Using 50.0 μmol of peptide, the free amino terminus was acylated with the oxycodone analog (20 mg, 50 μmol, 1eq) in the presence of DIEA (8.6 μL, 5.0 μmol, 0.1 eq) and HTCU (21 mg, 50 μmol, 1eq) in DMF (5 mL) for 10 h. After acylation was judged complete by ninhydrin analysis, the resin bound peptide was washed thoroughly with CH_2Cl_2 and dried *in vacuo* for 4 h. The peptide was then reacted with 5% hydrazine in DMF (5 mL, v/v) to orthogonally remove the Dde protected side chain. After verifying that deprotection was complete by ninhydrin analysis, the peptide was washed with CH_2Cl_2, dried, and then reacted with Biotin-Peg_4-SE (44 mg, 75 μmol, 1.5eq) in the presence of DIEA (8.6 μL, 5.0 μmol, 0.1 eq) in DMF (5 mL) 1eq. After biotinylation was judged complete by ninhydrin testing, the peptide was cleaved from the resin along with simultaneous side chain deprotection by treatment with Reagent K containing TFA (10 mL), crystalline phenol (0.5 g), 1,2-ethanedithiol (0.25 mL), thioanisole (0.5 mL), and H_2O (0.5 mL) for 2 h at rt. The released peptide was collected and combined with TFA washes of the resin before precipitation of the peptide in chilled Et_2O (100 mL). The crude solid peptide was collected by centrifugation, the supernatant was removed, and the resulting pellet was washed 2 times with cold Et_2O (50 mL) repeating the centrifugation and supernatant removal steps each time. The crude peptide was purified using a semipreparative C_{18} RP-HPLC column with detection at 214 nm and eluted with a gradient of Solvent A (H_20/0.1% TFA, v/v) and Solvent B (CH_3CN/0.1% TFA, v/v). The crude peptide (115 mg) was dissolved in a DMF/H_2O solution (1:5 v/v, 25 mL), applied to the column equilibrated in Solvent A, and eluted using a linear gradient of (0-70% Solvent B over 1.5 h at a flow-rate of 5 mL/min). Fractions were analyzed for purity with an analytical C_{18} RP-HPLC column employing a linear gradient (0-100% Solvent B over 60 min at a flow-rate of 1 mL/min) and detected at 214 nm. Fractions containing peptide product of at least 90% purity were pooled and concentrated by lyophilization to yield 23 mg (20% yield) of a white solid. A small amount (< 1mg) of the resulting purified peptide was dissolved in 10 μl of 0.1% TFA/CH_3CN and diluted 1:50 in a mixture of CH_3CN/H_2O (1:1 v/v) prior to MS analysis. MS was performed using a 50 μL injection and collecting 3000 scans. ESI-MS: calcd for $C_{108}H_{155}N_{25}O_{32}S$ $[M+2H]^{+2}$ 1173.0497, found 1173.0399.

Spleen biopsy

Sterile surgeries were performed under isofluorane anesthesia. Through a paramedian incision, the caudal portion of the spleen (∼50%) was resected and wounds sutured. Veterinary care consisted of 5mg/kg, s.c. Meloxicam (Boehringer Ingelheim, Fremont, CA) and 33mg/kg s.c. Rocephin (Sandoz, Princeton, NJ).

Immunization

Male BALB/c and C57Bl/6 mice (Harlan Laboratories, Madison, WI) were housed with a 12hr light /12 hr dark cycle, and fed *ad libitum*. In B cell studies, mice were immunized s.c. on days 0, 14 and 28 with 25 μg of either 6OXY-KLH or KLH absorbed to undiluted alum (Alhydrogel85, Brenntag Biosector, Frederikssund, Denmark) in a final volume of 0.2ml (25). In the CD4-depletion study, mice were administered anti-CD4 mAb (0.1 mg in PBS, i.p.), for three consecutive days prior to the first immunization and then twice weekly for the duration of the study (29). The rat IgG2b mAb against mouse CD4 was produced from hybridoma GK1.5 cells (ATCC, Rockville, MD). In the carrier-specific $CD4^+$ T cell study,

mice were immunized s.c. with 25 μg of 6OXY-OVA^{2W} absorbed to undiluted alum on days 0, 14 and 28.

Oxycodone-specific serum antibody titers

The 6OXY-specific serum IgG antibody titers were measured by ELISA (25). The 6OXY-specific serum IgG antibodies selectively bind oxycodone, hydrocodone and oxymorphone (24; 25; 30).

Vaccine efficacy on oxycodone antinociception and distribution

A week after the last immunization, mice were injected s.c. with 2.25 mg/kg oxycodone and antinociception was tested on a hot plate set at 54°C to determine the following behavioral endpoints: hind paw lifts and flicks, or reaching a maximal cutoff of 60 sec to avoid tissue damage (25). The % maximal possible effect (MPE %) was calculated as: (post-drug latency - baseline latency)/(maximal cutoff - baseline latency) × 100 (25). After the hot plate test, mice were euthanized by CO_2, and serum and brain oxycodone concentrations measured by gas chromatography coupled to mass spectrometry (25). Concentrations represent the total of protein-, antibody-bound and free drug in each sample.

Enrichment of hapten-specific B cells in spleen biopsy and blood samples

Partial spleen samples were collected from each mouse, and disaggregated as described(23). Whole blood was harvested by facial vein puncture, collected in tubes containing heparin 50 USP units (Hospira, NDC) and processed using the ammonium-chloride-potassium (ACK) lysing buffer (Lonza, NJ). Single-cell suspensions from each mouse were centrifuged at 1600 RPM for 5 min at 4°C and resuspended to a final volume of 200 μl sorter buffer (DPBS + 2% fetal bovine serum, 0.1% sodium azide) including Fc block (2.4G2, 2% rat serum, 0.1% sodium azide, BioXCell, West Lebanon, NH). Either PE-AF647 or (control peptide)$_4$-SA-PE-AF647 were added at a final concentration of 5 nM and incubated at room temperature for 5 min. The (6OXY)$_n$-PE or the (6OXY)$_4$-SA-PE conjugate were then added at concentration of 5 nM and incubated for 25 min at 4°C. Samples were washed in ice-cold sorter buffer, resuspended to a final volume of 200 μl of sorter buffer, mixed with 25 μl of anti-PE conjugated magnetic beads (Miltenyi Biotech, Inc, Auburn, CA) and incubated for 15 min at +4°C. The cells were resuspended in sorter buffer and passed through a magnetized LS column (Miltenyi Biotech). For each sample, bound fractions were collected, while flowthrough fractions were used for calibration and compensation. Fractions were centrifuged at 1600 RPM for 5 min at 4°C and resuspended in 100 μl of sorter buffer as described previously (20; 23). From each individual mouse partial splenectomy or blood sample, fluorescent counting beads (Accucheck, Invitrogen, Frederick, MD) were used to calculate total numbers of live lymphocytes, B cells and hapten-specific B cells in the bound fraction (23).

B cell staining

Cell suspensions were incubated with fluorochrome labeled anti-mouse antibodies for the following B cell surface markers: FITC anti-GL7, PE-Cy7 anti-B220, APC anti-IgM, AF700 anti-CD38, eF450 anti-IgD; and for the following APC-eF780 labeled anti-mouse antibodies

for non-B cell surface markers: anti-CD90.2, anti-CD11c, anti-Ly-6G and anti-F4/80. All antibodies were from eBioscience (San Diego, CA) with the exception of FITC anti-GL7 (BD Pharmingen). Cells were fixed in formaldehyde (Cytofix/Cytoperm, BD biosciences, San Diego, CA), washed with permeabilization buffer (BD biosciences, San Diego, CA), and incubated with the Pacific Orange labeled surface/ intracellular marker anti-mouse anti-Ig heavy and light chain (Invitrogen) as described (20).

Gating strategy for 6OXY-specific B cells

The gating strategy used to analyze 6OXY-specific B cells was previously described in detail (23). Total B cells were gated as cells that express immunoglobulin positive (Ig^{+}) but not the non-B cell markers CD90.2 (T cells), Gr-1 (neutrophils), CD11.c (dendritic cells) and F4/80 (macrophages). B cells binding the 6OXY hapten are distinguished from B cells bound to the PE-based decoys by comparing fluorescence between $(6OXY)_n$-PE and PE-AF647, or $(6OXY)_4$-SA-PE and $(\text{control peptide})_4$-SA-PE-AF647. 6OXY-specific B cells were identified as either $B220^{high}$ non-antibody secreting cells or Ig^{high} antibody-secreting cells (ASC). In contrast, the $B220^{neg}$ Ig^{MID} cells were excluded from B cell analysis (23), because this population consisted of non-B cells that bound circulating antibody via Fc receptors (31). 6OXY-specific $B220^{high}$ B cells were classified as $CD38^{low}$ $GL7^{high}$ germinal center (GC) or $CD38^{high}$ naïve and memory B cells. $CD38^{high}$ $GL7^{neg}$ B cells were further identified as IgM^{high} B cells, or as IgM^{neg} and IgD^{neg} switched immunoglobulin (swIg) B cells as described (20; 23). When specified, 6OXY-specific GC B cells were quantified as $CD38^{+}$ $GL7^{high}$ or $CD38^{neg}$ $GL7^{high}$ B cells as described (22), and shown in Supplemental Figure 2. We have previously shown that enriched 6OXY-specific B cells are specific for free oxycodone and hapten (23).

T cell analysis

Tissue samples were disaggregated to obtain a single-cell suspension. For $CD4^{+}$ and $CD8^{+}$ analysis, samples were directly labeled for T and non-T surface markers as described below. For detection of 2W1S-specific $CD4^{+}$ T cells, samples were first co-incubated with 10nM of 2W1S:I-A^{b}-PE, 2W1S:I-A^{b}-APC and BV421 anti-CXCR5 for 60 minutes at room temperature (27), washed, mixed with anti-PE and anti-APC magnetic beads and isolated through magnetic enrichment (27). Enriched single-cell suspensions were labeled with PE-Cy7 anti-CD45R, PE-Cy7 anti-CD11b, PE-Cy7 anti-CD11c, PE-Cy7 anti-F4/80, PE anti-CD4, BV510 anti-CD8a, APC-eFluor780 anti-CD4, PerCP-eFluor710 anti-CD90.2, FITC antiCD279, and AF700 anti-CD44. Using a flow cytometer, after identification of singlets through standard FSC-W and FSC-A gating, T cells were first identified as $CD90.2^{high}$, and then as $CD8^{high}$ T cells or $CD4^{high}$ T cells (27). Within the $CD4^{high}$ T cells, 2W1S-specific $CD4^{+}$ T cells were identified as PE^{high} and APC^{high} (27). Within the 2W1S-specific T cell gate, we identified $CXCR5^{high}$ T cells (27). However, $CD4^{+}$ $CXCR5^{high}$ T follicular helper cells are not usually found in the spleen of naïve mice, but here served as a site-specific population-specific internal negative control. T cell numbers were quantified using fluorescent counting beads (Accucheck, Invitrogen, Frederick, MD), while compensation was performed using Ultracorp eBeads (eBiosciences, San Diego, CA).

Flow cytometry—B and T cell analyses were performed on a 4-laser (355 nm, 405 nm, 488 nm, 633 nm) LSR II Fortessa using FACSDiva 7.0 (BD Biosciences), and processed with FlowJo (Tree Star, Ashland, OR).

Statistical analysis

6OXY-specific B cell numbers, oxycodone concentrations, and MPE% were compared by two-sided paired or unpaired T test within- or between- groups. 6OXY-specific B cells across groups were compared by one-way ANOVA followed by Tukey's post hoc test. The relationship between the 6OXY-specific B cells, $CD4^+$ T cells, carrier-specific $CD4^+$ T cells and 6OXY-specific titers, oxycodone concentrations and oxycodone MPE% within each group was analyzed by either Pearson or Spearman correlation after performing the D'Agostino and Pearson omnibus normality test. Analyses were performed using Graph Pad 6.0 (La Jolla, CA).

Results

The hapten-specific B cell population before and after immunization

To test the hypothesis that the initial size of the polyclonal hapten-specific B cell population determines vaccine efficacy, we analyzed B cells in naïve and immunized mice using fluorescent antigen-based magnetic enrichment paired with flow cytometry (23). In two independent studies, the 6OXY-specific B cell repertoire was analyzed in either spleen biopsy or blood samples collected before and after immunization with 6OXY-KLH or unconjugated KLH in alum (Figure 1A). Immunized mice were tested for serum antibodies, vaccine effect on oxycodone distribution to serum and to the brain, and oxycodone-induced behavior. In the cohort of mice that was analyzed by partial splenectomy at day 35, we determined 6OXY-specific serum IgG titers (Figure 1B) and their functional effects following injection with oxycodone (2.25 mg/kg, s.c.). This dose of oxycodone elicits maximal responses in the hot plate analgesia test providing an effective strategy to screen vaccine efficacy against opioids (25; 28). As expected, immunization with 6OXY-KLH increased serum oxycodone concentrations (Figure 1C), reduced distribution of oxycodone to the brain and oxycodone antinociception (Figure 1D, E).

Having determined that partial splenectomy did not interfere with the 6OXY-KLH efficacy, and knowing that partial splenectomy did not interfere with the IgM^{high} memory B cell population in mice (32), we took advantage of this approach to test the extent to which vaccine efficacy against oxycodone correlated to the naïve and early-activated 6OXY-specific B cell populations. In spleen biopsy samples from naive mice, we detected a substantial number of 6OXY-specific $B220^{high}$ $GL7^{-}$ $CD38^{high}$ IgM^{high} B cells (2,950±455, mean±SEM), but very low numbers of 6OXY-specific $B220^{high}$ $GL7^{-}$ $CD38^{high}$ IgM^{neg} IgD^{neg} swIg B cells, $B220^{high}$ $CD38^{low}$ $GL7^{high}$ GC B cells, or 6OXY-specific $B220^{low}$ Ig^{high} ASC B cells (Figure 2). 6OXY-specific ASC B cells were detected 14 days after the first immunization, but this response waned by day 35 (Figure 2A, B). Multiple immunizations with 6OXY-KLH increased 6OXY-specific GC and swIg B cells (Figure 2A, C, D). In contrast, no differences were detected in the number of 6OXY-specific IgM^{high} B cells before and after immunization (Figure 2A, E). Longitudinal B cell analysis by spleen

biopsy showed that 6OXY-KLH elicits 6OXY-specific GC and swIg B cells, which are critical for generation of long-term plasma and memory B cell responses.

Number of hapten-specific B cells prior to immunization dictates conjugate vaccine efficacy

Vaccine efficacy depends on adequate levels of serum antibodies that bind oxycodone in serum, thus preventing oxycodone distribution to the brain and oxycodone-induced behaviors (24; 25). Thus, we tested the extent to which the number of hapten-specific B cells prior to immunization correlated with vaccine efficacy. After spleen biopsies, the first cohort of naïve BALB/c mice (n=24) was randomly assigned to either the 6OXY-KLH or KLH immunization groups. The number of 6OXY-specific B cells was not different, in spleen biopsy samples, between the two groups prior to immunization (Supplemental Figure 1.A-C). As expected, immunization with 6OXY-KLH absorbed on alum significantly increased serum oxycodone concentrations after oxycodone administration (Supplemental Figure 1.D). Retention of oxycodone in serum correlated with the appearance of 6OXY-specific serum IgG antibodies after immunization (Figure 3A), as previously described in spleen-intact mice and rats (24; 25). Interestingly, a higher number of 6OXY-specific IgM^{high} and swIg B cells prior to immunization correlated to greater 6OXY-specific serum IgG titers 7 days after the last immunization (Figure 3B and C). In contrast, no relationship was found between the 6OXY-specific GC or ASC B cells prior to immunization and antibodies (not shown).

There was a trending association between increased levels of 6OXY-specific serum IgG antibodies and decreased distribution of oxycodone to the brain (Figure 3D). Strikingly, a higher number of 6OXY-specific IgM^{high} B cells prior to immunization correlated to lower brain oxycodone concentrations in the 6OXY-KLH group (Figure 3E). In contrast, no significant relationship was found between 6OXY-specific swIg (Figure 3F, r^2=0.28, p= 0.08), GC or ASC B cells prior to immunization and brain oxycodone in vaccinated mice (not shown). These data showed that the presence of a higher number of hapten-specific IgM^{high} B cells, and to a less extent swIg B cells, prior to immunization correlated to greater antibody titers and vaccine efficacy, supporting our hypothesis that the initial number of hapten-specific B cells underlies individual responses to vaccines. As a cautionary note, three or four individual data points may have contributed to determine the significant relationship between hapten-specific IgM^{high} and swIg B cells and vaccine effects (Figure 3). However, all data points were included in the statistical analysis because our study focused on individual variability in response to vaccines and the relationship between B cells and multiple independent parameters of vaccine efficacy. The lack of association between antibody titers or vaccine efficacy and numbers of 6OXY-specific GC or ASC B cells prior to immunization is consistent with the notion that these B cell phenotypes are generated only after vaccination.

Early hapten-specific GC and ASC B cells dictated vaccine immunogenicity or efficacy

Immunization with 6OXY-KLH increased the number of 6OXY-specific GC B cells in the spleen compared to KLH and naïve groups (Figure 2C). Similarly, compared to naïve mice (Figure 4A), the ratio between 6OXY-specific GC B cells and other B cell phenotypes changed 14 days after vaccination (Figure 4B). Individual distributions of B cell subsets

(e.g., the ratio between GC:IgM^{high}:swIg:ASC) were qualitatively different suggesting variable GC responses, which may underlie individual differences in vaccine efficacy.

To better understand the polyclonal B cell responses to 6OXY-KLH and to test whether vaccination elicits characteristic GC activation, we further characterized 6OXY-specific GC B cells as "GC-independent" CD38^{+} GL7^{high} or "GC-dependent" CD38^{-} GL7^{high} B cells (22). Prior to immunization, 6OXY-specific CD38^{+} GL7^{high} B cells generally out-numbered CD38^{-} GL7^{high} B cells (451±73 vs 107±23, mean±SEM, $p<0.001$; Supplemental Figure 2). In contrast, immunization with 6OXY-KLH specifically increased the number of 6OXY-specific CD38^{-} GL7^{high} B cells compared to KLH and naïve groups (Supplemental Figure 2), thus increasing the ratio of CD38^{-} GL7^{high} over CD38^{+} GL7^{high} B cells (Figure 4C), which reflects GC activation.

In the cohort of mice analyzed by spleen biopsy 14 days after the first immunization, 6OXY-KLH effectively increased serum oxycodone concentrations (Figure 4D). There was also greater GC activation, as shown by the increased ratio of 6OXY-specific CD38^{-} to CD38^{+} GL7^{high} GC B cells in individual mice, correlating with greater efficacy on oxycodone serum distribution (Figure 4E). In fact, increased number of 6OXY-specific CD38^{-} GL7^{high} B cells ($r=0.73$, $p<0.0001$, not shown) and 6OXY-specific Ig^{high} B cells (Figure 4F) 14 days after immunization correlated with greater subsequent efficacy in increasing serum oxycodone concentrations at 35 days. Collectively, these data support our hypothesis that the size of the early-activated hapten-specific B cell population contributes to the conjugate vaccine efficacy.

Blood 6OXY-specific B cells correlate to vaccine efficacy

To test translational validity, we studied the extent to which the size of the 6OXY-specific B cell population in blood correlated to vaccine efficacy against oxycodone. To identify rare high affinity 6OXY-specific B cells in small blood volumes, we have developed an enrichment reagent consisting of the 6OXY hapten conjugated to a short biotinylated peptide, bound to PE-conjugated streptavidin (SA-PE), which provided the $(6OXY)_4$-SA-PE fluorescent conjugate of known haptenization ratio. Using this tool, we analyzed the frequency of polyclonal 6OXY-specific B cells in the blood of a cohort of BALB/c mice (n=24) before and after immunization with either 6OXY-KLH or KLH in alum. Immunization was effective in decreasing brain oxycodone (Figure 5A), and the increased blockage of brain oxycodone was dependent on early generation of serum antibody titers against oxycodone (Figure 5B). Instead, an increased frequency of 6OXY-specific IgM^{high} B cells in enriched blood samples collected prior to immunization correlated with greater vaccine efficacy in blocking oxycodone brain distribution in mice (Figure 5C). Furthermore, immunization with 6OXY-KLH increased the blood frequency of 6OXY-specific IgM^{high}, swIg and GC B cells compared to the KLH control group (Figure 5D-F). In contrast, 6OXY-specific ASC B cells were barely detected in blood before or 14 days after immunization. Analysis of 6OXY-specific B cells in blood was performed 14 days after immunization to be consistent with analysis performed by spleen biopsy (Figure 1-4) and our previous report (23).

An increased frequency of 6OXY-specific IgM^{high} B cells in enriched blood samples collected 14 days after immunization correlated with subsequent greater vaccine effect on oxycodone distribution to serum (Figure 5G), brain (Figure 5H) and prevention of oxycodone behavioral effects (Figure 5I). A similar significant relationship was found between 6OXY-specific GC and swIg B cells and vaccine efficacy (Supplemental Figure 3). The association between vaccine efficacy and 6OXY-specific B cells either before or shortly after immunization supports the hypothesis that naïve and early-activated hapten-specific B cells are derived from the same B cell compartment, and that the initial size of the 6OXY-specific B cell population correlates to vaccine success.

T cell-dependent B cell activation is necessary for vaccine efficacy

To further support the finding that early B cell clonal expansion 14 days after immunization dictated subsequent therapeutic effects at day 35, we tested 6OXY-KLH efficacy following $CD4^+$ T cell depletion in C57Bl/6 mice (n=6 each group). Anti-CD4 mAb-mediated selective depletion of $CD4^+$ T cells (Figure 6A) led to decreased frequency of 6OXY-specific IgM^{high} and swIg B cells in blood (Figure 6B). In this study, 6OXY-specific ASC and GC B cells were not detected after immunization (not shown), which reflected the observed overall lower frequencies of 6OXY-specific B cells in enriched blood from C57Bl/6 mice compared to BALB/c. As expected, $CD4^+$ T cell depletion blunted vaccine efficacy against oxycodone (Figure 6C).

Then, we tested the extent to which the population size of carrier-specific T cells related to vaccine efficacy. To analyze carrier-specific naïve $CD4^+$ T cells, we used a peptide:MHC II tetramer-based enrichment method (33). This strategy has been previously used to track antigen-specific T cells during the course of a bacterial infection in mice (34). Prior to immunization, by means of spleen biopsy, we determined the number of $CD4^+$ T cells specific for the 2W1S variant of $peptide_{52\text{-}68}$ epitope from the I-Eα chain (33). We then immunized C57Bl/6 mice with the 6OXY-OVA labeled with the 2W1S peptide (6OXY-OVA^{2W}, n=9). As expected, higher numbers of 2W:I-A^b-specific $CD4^+$ T cells prior to immunization were tightly correlated to vaccine efficacy (Figure 6D). These data suggest that 6OXY-specific B cells and carrier-specific $CD4^+$ T cells were highly interrelated and both contributed to vaccine efficacy.

Murine 6OXY-specific B cells frequencies across tissues

Before vaccination, the frequency of 6OXY-specific B cell subsets among total B cells in the enriched bound fraction (Figure 7A-D) was consistent across spleen biopsy, blood and the previously analyzed pooled peripheral lymph nodes and spleen samples (23). The 6OXY-specific B cell repertoire consisted mainly of IgM^{high} B cells (Figure 7). From the total B cells detected in enriched spleen biopsy samples (246,600±32,000, mean±SEM, n=23 mice), 1.5±0.2% were 6OXY-specific IgM^{high} B cells (2,950±455, mean±SEM); while 6OXY-specific IgM^{high} B cells constituted 0.8±0.12% of total B cells in lymph nodes and spleen samples (Figure 7A). From the total B cells detected in enriched blood samples (5,440±610, mean±SEM, n=24 mice), 2.2±0.3% were 6OXY-specific IgM^{high} B cells (125±20, mean±SEM, n=24). These data showed that analysis of hapten-specific B cells can be performed in various tissues, including peripheral blood, prior to immunization.

Discussion

The translation of therapeutic vaccines against drug addiction has been slow because clinical efficacy is achieved only in the small subset of immunized subjects that showed the highest levels of drug-specific serum antibodies. Previously, we found that a greater number of hapten-specific B cells correlated to greater efficacy of oxycodone vaccines consisting of conjugate immunogens containing different structurally-related haptens (23) or administered in different adjuvant formulations (28). Here, we hypothesized that clinically significant responses to addiction vaccines may be predicted from the number of hapten-specific B cells in unimmunized subjects and by the number of activated hapten-specific B cells present soon after immunization. Using an antigen-based enrichment strategy paired with flow cytometry analysis, we found that a higher frequency of naïve and early-activated hapten-specific B cells in spleen biopsies and blood correlated with subsequent greater vaccine efficacy against oxycodone. Additionally, $CD4^+$ T cell-dependent B cell activation was required for vaccine efficacy and the number of carrier-specific $CD4^+$ T cells prior to immunization correlated with vaccine efficacy. Our data suggest that vaccine clinical efficacy may be increased by analyzing blood from patients for the presence of hapten-specific B cells to determine which subjects are most likely to benefit from vaccination. This strategy may help physicians to personalize vaccine-based therapy, or to monitor clinical trials at early stages. Although more studies are needed before extending these results beyond addiction vaccines, it is tempting to speculate that the efficacy of other therapeutic vaccines containing haptens derived from tumor-associated small carbohydrate and peptide antigens, or Alzheimer's β amyloid-derived peptides may be similarly influenced and predicted by the number of antigen-specific B cells at the time of vaccination.

We have previously shown that a single immunization with the 6OXY-KLH immunogen selectively increased the polyclonal hapten-specific B cell population in pooled peripheral lymph nodes and spleen (23). In the current study, one immunization or multiple boosts with 6OXY-KLH in alum adjuvant increased the polyclonal hapten-specific B cell population, which includes the ASC, GC, IgM^{high} and swIg B cell subsets, in either the spleen or blood compartments which is consistent with previous analysis (23), and reports of NP-specific B cells in mice immunized with NP-KLH (35) or PE-specific B cells in mice immunized with PE (22). These results suggest that immunization with 6OXY-KLH in alum adjuvant induces GC formation, and plasma and memory B cells, supporting previous evidence of pre-clinical efficacy.

In the spleen, an increased number of hapten-specific IgM^{high} naïve and memory B cells, and at least in part switched memory B cells, before immunization correlated to greater post-vaccination antibody responses and vaccine efficacy in blocking distribution of oxycodone to the brain. Also in spleen, the numbers of 6OXY-specific GC and ASC B cells shortly after immunization correlated to subsequent vaccine efficacy. In blood, the presence of increased numbers of 6OXY-specific IgM^{high} B cells before immunization, or 6OXY-specific IgM^{high}, GC and swIg B cells at two weeks after vaccination, correlated to increased vaccine ability to prevent brain distribution and block oxycodone antinociception. These results, summarized in supplemental Table I, suggest that the frequencies of 6OXY-specific IgM^{high} and swIg B cell subsets are the best predictors of vaccine efficacy.

Moreover, these data suggest that the initial size of the polyclonal hapten-specific naïve B cell population correlates to the size of the early-activated B cell population shortly after vaccination which, during GC formation, determines the magnitude of the antibody response against oxycodone and vaccine efficacy. Our study is supported by findings that various pre-immunization serologic, transcriptomic, and cellular parameters in human blood, including the frequency of B cell subsets, were stable over time and correlated with antibody responses in subjects immunized with seasonal and pandemic influenza vaccines (36). The hypothesis that vaccine-specific B cells may provide predictive biomarkers of vaccine efficacy is further supported by a correlation found between switched memory B cells in human peripheral blood mononuclear cells (PBMC) and the efficacy of an H1N1 influenza vaccine (37).

Immunization with 6OXY-KLH increased GC B cells, and a more detailed analysis of GC B cells in spleen biopsies revealed that 6OXY-KLH stimulated expansion of “genuine” $CD38^{neg}$ $GL7^{high}$ GC B cells, which is a hallmark of longer-lived switched immunoglobulin memory B cell through GC formation (22). In contrast, generation of $CD38^{+}$ $GL7^{high}$ B cells is a critical feature of GC-independent memory formation, which leads to differentiation in IgM^{high} and shorter-lived switched immunoglobulin memory B cells (22). The presence of $CD38^{neg}$ $GL7^{high}$ GC B cells after immunization supports the 6OXY-KLH's ability to generate switched immunoglobulin memory B cells rather than IgM^{high} B cells. In fact, increased GC activation and the frequency of hapten-specific GC B cells tightly correlated to vaccine efficacy against oxycodone. These data suggest that the lack of addiction vaccine efficacy in patients displaying low antibody titers is not due to GC-independent hapten-specific B cell responses. Rather, these data indicate that after immunization, variability in the timing, quality and magnitude of GC activation might underlie individual differences in therapeutic vaccine efficacy against drugs of abuse or other small molecules.

Selective depletion of $CD4^{+}$ T helper cells in secondary lymphoid organs prevented activation of hapten-specific B cells and blunted vaccine efficacy. These results suggest that a large number of naïve and early-activated hapten-specific B cells, in the presence of a sizeable carrier-specific $CD4^{+}$ T cell population, may be required for optimal T cell-dependent B cell activation and vaccine efficacy against oxycodone. Indeed, using carrier proteins labeled with known T cell epitopes and peptide:$I\text{-}A^{b}$ tetramers, to study naïve $CD4^{+}$ T cells, we found that the initial population of carrier-specific $CD4^{+}$ T cells prior to immunization correlated to vaccine efficacy against oxycodone. Overall, our results are consistent with findings that increased numbers of GC B cells are correlated to, and necessary for, increased antigen-specific TfH cell responses (38; 39). However, the novelty of our study is that we have established a relationship between the polyclonal hapten-specific B cell and carrier-specific $CD4^{+}$ T cell populations and vaccine efficacy in wild-type BALB/c and C57Bl/6 mice.

Here, we reported a correlation between the size of the polyclonal naïve and early-activated hapten-specific B cell populations and subsequent measures of vaccine efficacy against oxycodone. In this study, we have focused on vaccine's effects shortly (7 days) after the last immunization to be consistent with our previous vaccine development work (24-26; 28).

Clinical evaluation of nicotine and cocaine vaccines involved immunization regimens of 3 to 5 monthly doses followed by booster injections every 2 or 6 months to maintain high serum antibody levels, showing half-lives of ∼2-3 months (6; 7; 40). In future investigations, it will be important to address how the frequency of naïve hapten-specific B cells, or alternatively carrier-specific $CD4^+$ T cells, influences long-term adaptive immune responses to vaccines against drugs of abuse.

The current findings, and the reported methods for analysis of antigen-specific B and T cells, may aid the development of novel mechanism-based strategies to increase the overall efficacy of vaccines against drugs of abuse. Analysis of hapten-specific B cells and carrier-specific $CD4^+$ T cells may speed vaccine discovery by screening the lead haptens that best bind B cells, novel vaccine carriers and delivery platforms that enhance stimulation of T cell help, or by comparing candidate conjugate immunogens to predict their likelihood of clinical efficacy.

Using our enrichment strategy, hapten-specific B cells were easily detected in mouse blood before and after immunization. Application of this approach to human PBMC may inform development of therapeutic vaccines suitable for human testing and companion diagnostic tests to identify patients that will likely respond to vaccine therapy. Indeed, B cell-based predictive biomarkers may aid patient stratification and design of adaptive clinical trials. The clinical benefit of such strategies is supported by evidence that pre-existing serum antibodies for a blood group determinant and a viral glycan correlated with overall survival in patients immunized with a candidate prostate cancer vaccine (41; 42). Analysis of the vaccine-specific B and T cell repertoire may be combined with high-throughput immune repertoire sequencing (43) to accelerate development of vaccines against chronic non-communicable diseases.

Supplementary Material

Refer to Web version on PubMed Central for supplementary material.

Acknowledgments

The authors thank MMRF for purchasing a BD Biosciences LSRIIFortessa, Marc Jenkins group for providing the 2W1S:I-A^b tetramers and critical support, and Paul Pentel for helpful discussion. The authors also thank Maria Luisa Gelmi for establishing an institutional and educational agreement between the Facolta di Scienze Farmacologiche, Universita degli Studi di Milano, Italy and the University of Minnesota Medical School, Minneapolis, Minnesota.

This work was supported by NIH DA034487 and MMRF Translational Research Award (Pravetoni).

References

1. Rappuoli R, Pizza M, Del Giudice G, De Gregorio E. Vaccines, new opportunities for a new society. Proc Natl Acad Sci U S A. 2014; 111:12288–93. [PubMed: 25136130]
2. Pentel PR, LeSage MG. New directions in nicotine vaccine design and use. Adv Pharmacol. 2014; 69:553–580. [PubMed: 24484987]
3. Shen XY, Orson FM, Kosten TR. Vaccines against drug abuse. Clin Pharmacol Ther. 2012; 91:60–70. [PubMed: 22130115]

4. Astronomo RD, Burton DR. Carbohydrate vaccines: developing sweet solutions to sticky situations? Nat Rev Drug Discov. 2010; 9:308–324. [PubMed: 20357803]
5. Liu B, Frost JL, Sun J, Fu H, Grimes S, Blackburn P, Lemere CA. MER5101, a novel Abeta1-15:DT conjugate vaccine, generates a robust anti-Abeta antibody response and attenuates Abeta pathology and cognitive deficits in APPswe/PS1DeltaE9 transgenic mice. J Neurosci. 2013; 33:7027–7037. [PubMed: 23595760]
6. Hatsukami DK, Jorenby DE, Gonzales D, Rigotti NA, Glover ED, Oncken CA, Tashkin DP, Reus VI, Akhavain RC, Fahim RE, Kessler PD, Niknian M, Kalnik MW, Rennard SI. Immunogenicity and smoking-cessation outcomes for a novel nicotine immunotherapeutic. Clin Pharmacol Ther. 2011; 89:392–399. [PubMed: 21270788]
7. Martell BA, Orson FM, Poling J, Mitchell E, Rossen RD, Gardner T, Kosten TR. Cocaine vaccine for the treatment of cocaine dependence in methadone-maintained patients: a randomized, double-blind, placebo-controlled efficacy trial. Arch Gen Psychiatry. 2009; 66:1116–1123. [PubMed: 19805702]
8. Gilewski TA, Ragupathi G, Dickler M, Powell S, Bhuta S, Panageas K, Koganty RR, Chin-Eng J, Hudis C, Norton L, Houghton AN, Livingston PO. Immunization of high-risk breast cancer patients with clustered sTn-KLH conjugate plus the immunologic adjuvant QS-21. Clin Cancer Res. 2007; 13:2977–2985. [PubMed: 17504999]
9. Miles D, Roche H, Martin M, Perren TJ, Cameron DA, Glaspy J, Dodwell D, Parker J, Mayordomo J, Tres A, Murray JL, Ibrahim NK. Phase III multicenter clinical trial of the sialyl-TN (STn)-keyhole limpet hemocyanin (KLH) vaccine for metastatic breast cancer. Oncologist. 2011; 16:1092–1100. [PubMed: 21572124]
10. UNODC. World Drug Report 2013. 2013
11. CDC. Wide-ranging OnLine Data for Epidemiologic Research (WONDER). 2014
12. Dodrill CL, Helmer DA, Kosten TR. Prescription pain medication dependence. Am J Psychiatry. 2011; 168:466–471. [PubMed: 21536702]
13. Stotts AL, Dodrill CL, Kosten TR. Opioid dependence treatment: options in pharmacotherapy. Expert Opin Pharmacother. 2009; 10:1727–1740. [PubMed: 19538000]
14. Skolnick P, Volkow ND. Addiction therapeutics: obstacles and opportunities. Biol Psychiatry. 2012; 72:890–891. [PubMed: 23121867]
15. McHeyzer-Williams M, Okitsu S, Wang N, McHeyzer-Williams L. Molecular programming of B cell memory. Nat Rev Immunol. 2012; 12:24–34. [PubMed: 22158414]
16. Crotty S. Follicular helper CD4 T cells (TFH). Annu Rev Immunol. 2011; 29:621–663. [PubMed: 21314428]
17. Taylor JJ, Jenkins MK, Pape KA. Heterogeneity in the differentiation and function of memory B cells. Trends Immunol. 2012; 33:590–597. [PubMed: 22920843]
18. Jenkins MK, Moon JJ. The role of naive T cell precursor frequency and recruitment in dictating immune response magnitude. J Immunol. 2012; 188:4135–4140. [PubMed: 22517866]
19. Geiger R, Duhen T, Lanzavecchia A, Sallusto F. Human naive and memory CD4+ T cell repertoires specific for naturally processed antigens analyzed using libraries of amplified T cells. J Exp Med. 2009; 206:1525–1534. [PubMed: 19564353]
20. Pape KA, Taylor JJ, Maul RW, Gearhart PJ, Jenkins MK. Different B cell populations mediate early and late memory during an endogenous immune response. Science. 2011; 331:1203–1207. [PubMed: 21310965]
21. Taylor JJ, Martinez RJ, Titcombe PJ, Barsness LO, Thomas SR, Zhang N, Katzman SD, Jenkins MK, Mueller DL. Deletion and anergy of polyclonal B cells specific for ubiquitous membrane-bound self-antigen. J Exp Med. 2012; 209:2065–2077. [PubMed: 23071255]
22. Taylor JJ, Pape KA, Jenkins MK. A germinal center-independent pathway generates unswitched memory B cells early in the primary response. J Exp Med. 2012; 209:597–606. [PubMed: 22370719]
23. Taylor JJ, Laudenbach M, Tucker AM, Jenkins MK, Pravetoni M. Hapten-specific naive B cells are biomarkers of vaccine efficacy against drugs of abuse. J Immunol Methods. 2014; 405:74–86. [PubMed: 24462800]

24. Pravetoni M, Le Naour M, Harmon T, Tucker A, Portoghese PS, Pentel PR. An oxycodone conjugate vaccine elicits oxycodone-specific antibodies that reduce oxycodone distribution to brain and hot-plate analgesia. J Pharmacol Exp Ther. 2012; 341:225–32. [PubMed: 22262924]
25. Pravetoni M, Le Naour M, Tucker AM, Harmon TM, Hawley TM, Portoghese PS, Pentel PR. Reduced antinociception of opioids in rats and mice by vaccination with immunogens containing oxycodone and hydrocodone haptens. J Med Chem. 2013; 56:915–923. [PubMed: 23249238]
26. Pravetoni M, Pentel PR, Potter DN, Chartoff EH, Tally L, LeSage MG. Effects of an oxycodone conjugate vaccine on oxycodone self-administration and oxycodone-induced brain gene expression in rats. PLoS One. 2014; 9:e101807. [PubMed: 25025380]
27. Tubo NJ, Pagan AJ, Taylor JJ, Nelson RW, Linehan JL, Ertelt JM, Huseby ES, Way SS, Jenkins MK. Single Naive CD4(+) T Cells from a Diverse Repertoire Produce Different Effector Cell Types during Infection. Cell. 2013; 153:785–796. [PubMed: 23663778]
28. Pravetoni M, Vervacke JS, Distefano MD, Tucker AM, Laudenbach M, Pentel PR. Effect of Currently Approved Carriers and Adjuvants on the Pre-Clinical Efficacy of a Conjugate Vaccine against Oxycodone in Mice and Rats. PLoS One. 2014; 9:e96547. [PubMed: 24797666]
29. Norian LA, Kresowik TP, Rosevear HM, James BR, Rosean TR, Lightfoot AJ, Kucaba TA, Schwarz C, Weydert CJ, Henry MD, Griffith TS. Eradication of metastatic renal cell carcinoma after adenovirus-encoded TNF-related apoptosis-inducing ligand (TRAIL)/CpG immunotherapy. PLoS One. 2012; 7:e31085. [PubMed: 22312440]
30. Pravetoni M, Raleigh MD, Le Naour M, Tucker AM, Harmon TM, Jones JM, Birnbaum AK, Portoghese PS, Pentel PR. Co-administration of morphine and oxycodone vaccines reduces the distribution of 6-monoacetylmorphine and oxycodone to brain in rats. Vaccine. 2012; 30:4617–4624. [PubMed: 22583811]
31. Bell J, Gray D. Antigen-capturing cells can masquerade as memory B cells. J Exp Med. 2003; 197:1233–1244. [PubMed: 12756262]
32. Tracy ET, Haas KM, Gentry T, Danko M, Roberts JL, Kurtzberg J, Rice HE. Partial splenectomy but not total splenectomy preserves immunoglobulin M memory B cells in mice. J Pediatr Surg. 2011; 46:1706–1710. [PubMed: 21929978]
33. Moon JJ, Chu HH, Hataye J, Pagan AJ, Pepper M, McLachlan JB, Zell T, Jenkins MK. Tracking epitope-specific T cells. Nat Protoc. 2009; 4:565–581. [PubMed: 19373228]
34. Dileepan T, Linehan JL, Moon JJ, Pepper M, Jenkins MK, Cleary PP. Robust antigen specific th17 T cell response to group A Streptococcus is dependent on IL-6 and intranasal route of infection. PLoS Pathog. 2011; 7:e1002252. [PubMed: 21966268]
35. King IL, Fortier A, Tighe M, Dibble J, Watts GF, Veerapen N, Haberman AM, Besra GS, Mohrs M, Brenner MB, Leadbetter EA. Invariant natural killer T cells direct B cell responses to cognate lipid antigen in an IL-21-dependent manner. Nat Immunol. 2012; 13:44–50. [PubMed: 22120118]
36. Tsang JS, Schwartzberg PL, Kotliarov Y, Biancotto A, Xie Z, Germain RN, Wang E, Olnes MJ, Narayanan M, Golding H, Moir S, Dickler HB, Perl S, Cheung F. Global analyses of human immune variation reveal baseline predictors of postvaccination responses. Cell. 2014; 157:499–513. [PubMed: 24725414]
37. Frasca D, Diaz A, Romero M, Phillips M, Mendez NV, Landin AM, Blomberg BB. Unique biomarkers for B-cell function predict the serum response to pandemic H1N1 influenza vaccine. Int Immunol. 2012; 24:175–182. [PubMed: 22281510]
38. Baumjohann D, Preite S, Reboldi A, Ronchi F, Ansel KM, Lanzavecchia A, Sallusto F. Persistent antigen and germinal center B cells sustain T follicular helper cell responses and phenotype. Immunity. 2013; 38:596–605. [PubMed: 23499493]
39. Kitano M, Moriyama S, Ando Y, Hikida M, Mori Y, Kurosaki T, Okada T. Bcl6 protein expression shapes pre-germinal center B cell dynamics and follicular helper T cell heterogeneity. Immunity. 2011; 34:961–972. [PubMed: 21636294]
40. Cornuz J, Zwahlen S, Jungi WF, Osterwalder J, Klingler K, van Melle G, Bangala Y, Guessous I, Muller P, Willers J, Maurer P, Bachmann MF, Cerny T. A vaccine against nicotine for smoking cessation: a randomized controlled trial. PLoS One. 2008; 3:e2547. [PubMed: 18575629]

41. Campbell CT, Gulley JL, Oyelaran O, Hodge JW, Schlom J, Gildersleeve JC. Serum antibodies to blood group A predict survival on PROSTVAC-VF. Clin Cancer Res. 2013; 19:1290–1299. [PubMed: 23362327]

42. Campbell CT, Gulley JL, Oyelaran O, Hodge JW, Schlom J, Gildersleeve JC. Humoral response to a viral glycan correlates with survival on PROSTVAC-VF. Proc Natl Acad Sci U S A. 2014; 111:E1749–1758. [PubMed: 24733910]

43. DeKosky BJ, Kojima T, Rodin A, Charab W, Ippolito GC, Ellington AD, Georgiou G. In-depth determination and analysis of the human paired heavy- and light-chain antibody repertoire. Nat Med. 2015; 21:86–91. [PubMed: 25501908]

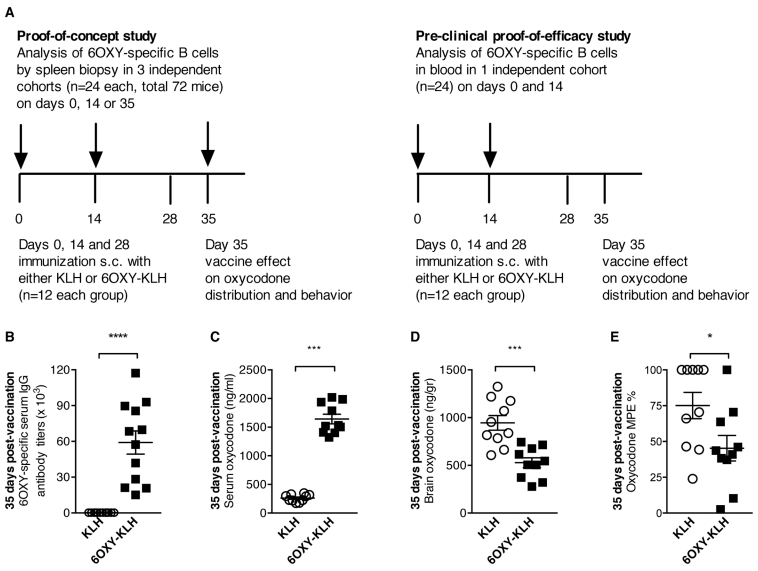

Figure 1. Study design and evaluation of vaccine efficacy

A) Analysis of 6OXY-specific B cells was performed either in spleen biopsy or blood samples before and after immunization with 6OXY-KLH or KLH in alum on days 0, 14 and 28 (n=12 each group). B-E) Shown data from a BALB/c mice cohort that received partial splenectomy a week after the third immunization. On day 35, 2.25 mg/kg s.c. oxycodone was administered to mice for testing vaccine's effect on oxycodone distribution to serum and to the brain, and on oxycodone nociception. B) 6OXY-specific serum IgG titers in mice immunized with 6OXY-KLH or unconjugated KLH. Effect of immunization on: oxycodone distribution to C) serum and D) the brain, and E) oxycodone antinociception. The maximum possible effect (MPE) represents hind paw lifts on a hot plate (25). *$p<0.05$ and ***$p<0.001$; brackets indicate group differences.

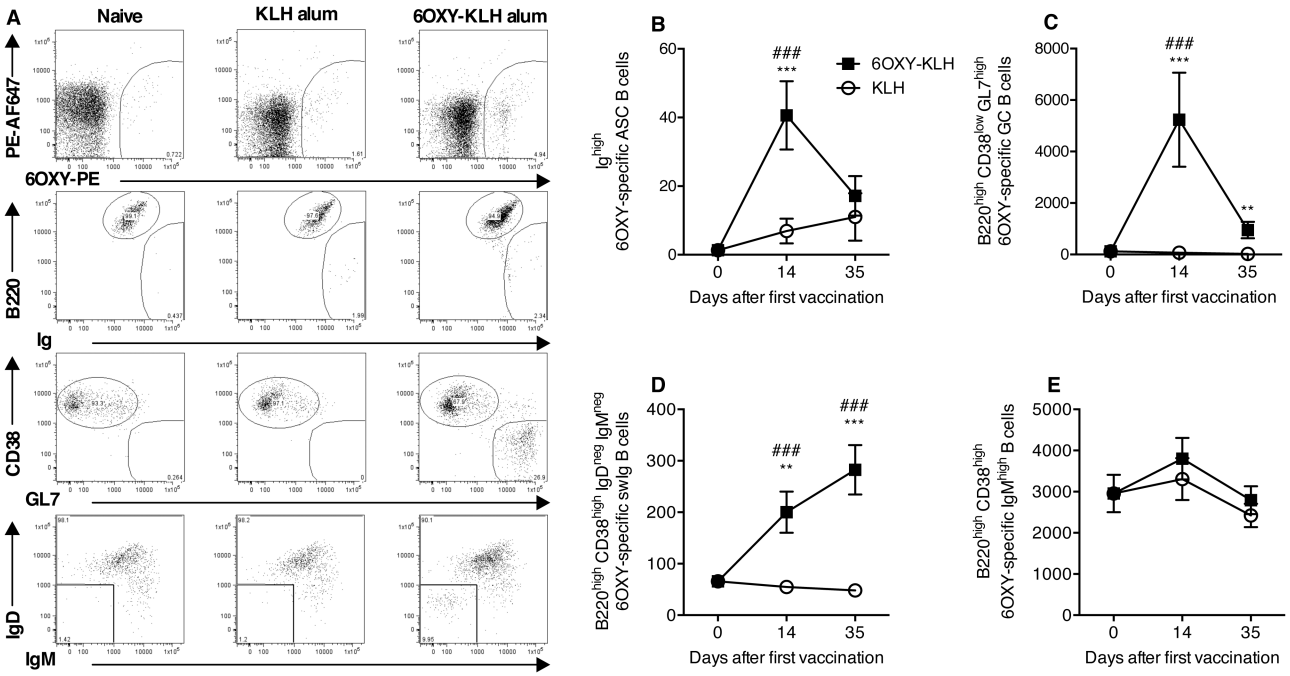

Figure 2. Splenic polyclonal hapten-specific B cells before and after immunization

6OXY-specific B cells were analyzed by spleen biopsy prior to immunization (n=24), 14 days after the first immunization and 7 days after the last immunization (n=12 mice each group). A) Representative flow cytometry plots of 6OXY-specific B cells in naïve mice, or mice immunized with either 6OXY-KLH or KLH. Data shown were collected on day 35. To analyze 6OXY-specific B cells, B cells bound to either $(6OXY)_n$-PE or PE-AF674 were positively isolated by magnetic enrichment (23). Using flow cytometry, B cells bound to $(6OXY)_n$-PE were distinguished and analyzed for B cell-specific markers (23). 6OXY-specific B cells were either $B220^{high}$ non-antibody secreting cells or Ig^{high} ASC B cells. 6OXY-specific $B220^{high}$ B cells were either $CD38^{low}$ $GL7^{high}$ GC or $CD38^{high}$ naïve and memory B cells. $CD38^{high}$ $GL7^{-}$ B cells were further identified as IgM^{high} or IgM^{neg} and IgD^{neg} swIg B cells (20; 23). 6OXY-specific B cells were B) ASC, C) GC, D) swIg B, and E) IgM^{high} naive and memory. Data shown are the number of 6OXY-specific B cells per spleen biopsy fragments. Data are mean±SEM. Each group is a composite of three independent experiments for a total n=24 before immunization and n=12 each group after immunization. *p<0.05, **p<0.01, and ***p<0.001 compared to KLH group; ### p<0.001 compared to naïve mice.

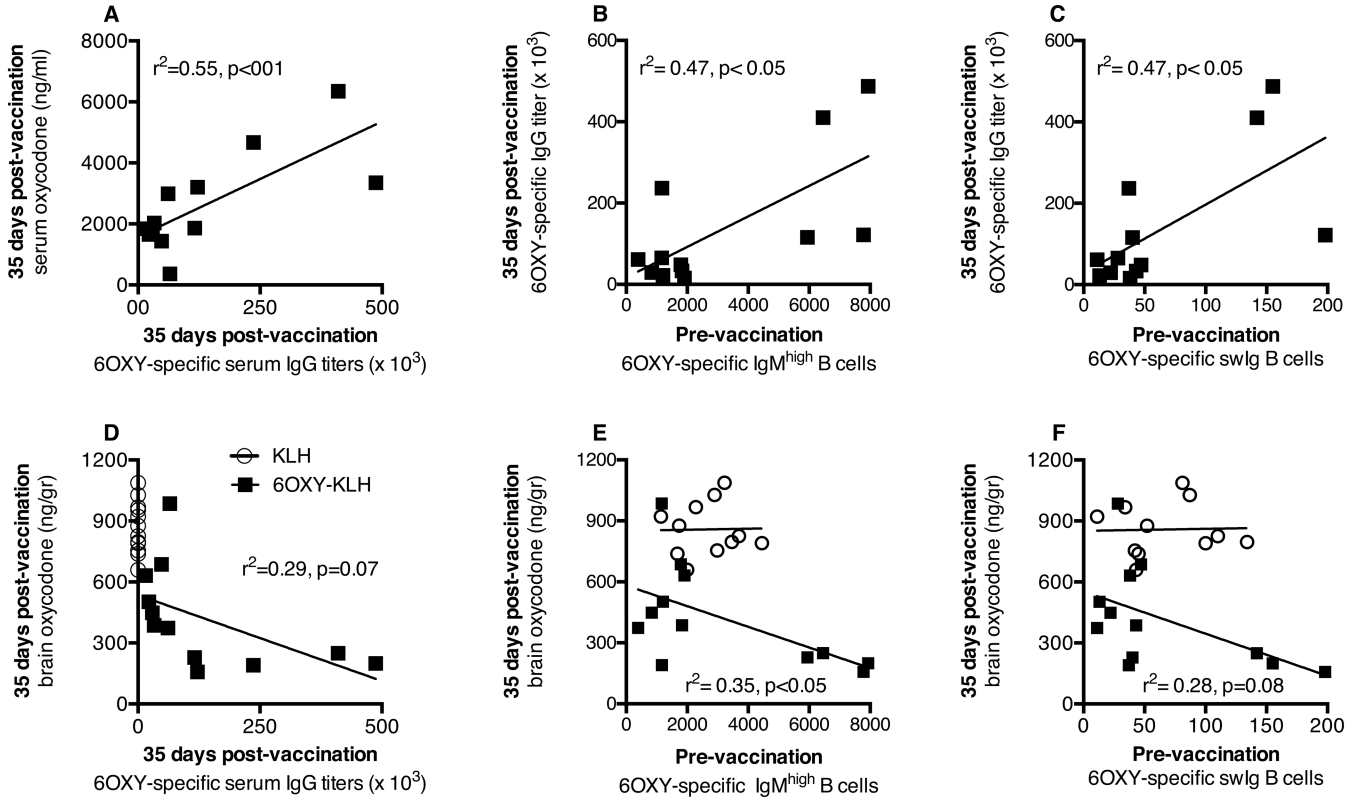

Figure 3. Number of splenic hapten-specific B cells prior to immunization correlated to vaccine efficacy

Pre-vaccination B cell analysis by spleen biopsy was performed in a naïve cohort of mice and then randomly immunized with either KLH or 6OXY-KLH (n=12 each group). Data shown are the number of 6OXY-specific B cells per spleen biopsy sample from individual mice. In mice immunized with 6OXY-KLH: A) 6OXY-specific serum IgG titers vs serum oxycodone, B) 6OXY-specific IgM^{high} B cells, and C) 6OXY-specific swIg B cells vs 6OXY-specific serum IgG titers. In mice immunized with 6OXY-KLH or KLH: D) 6OXY-specific serum IgG titers vs brain oxycodone, E) 6OXY-specific IgM^{high} B cells and F) 6OXY-specific swIg B cells vs brain oxycodone. Each group is a composite of three independent experiments with n=12 each immunization group.

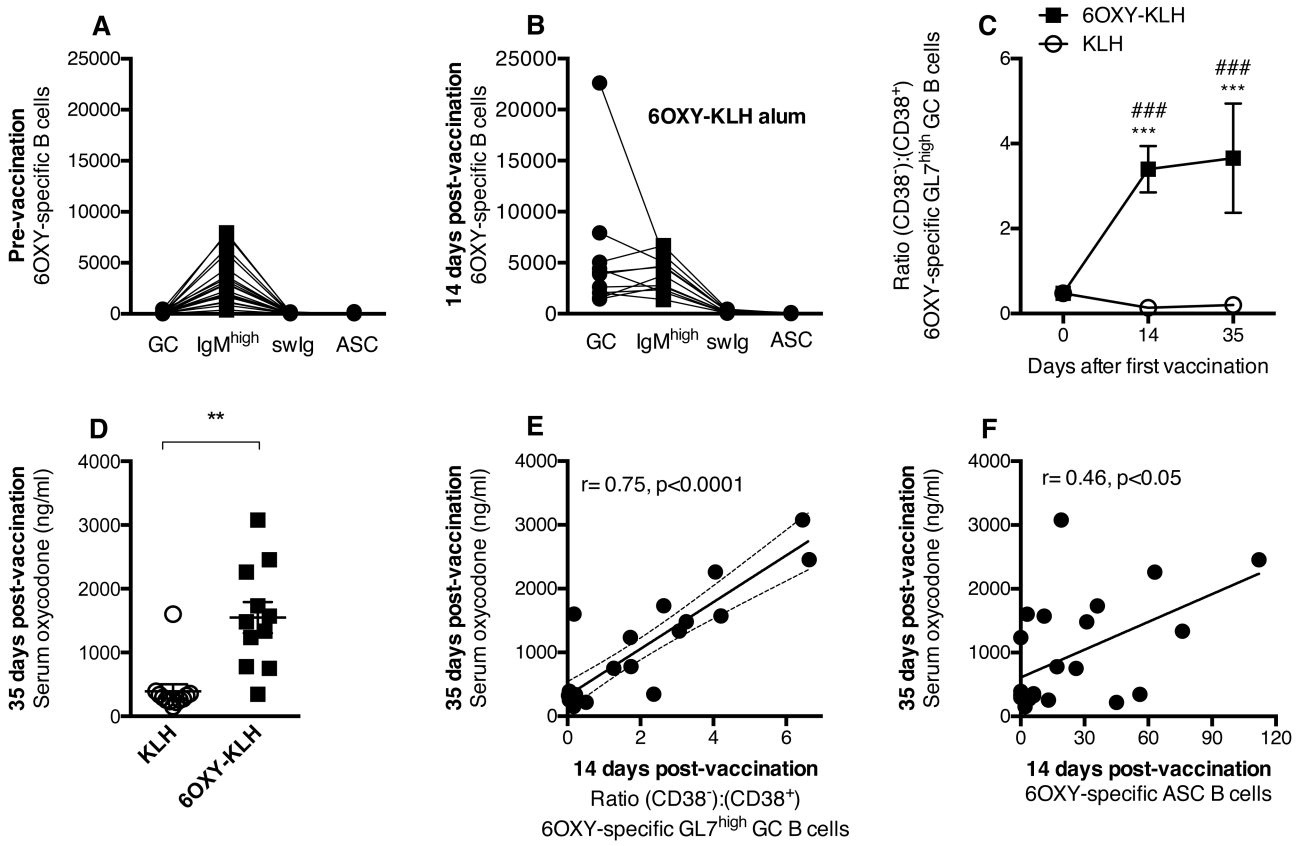

Figure 4. Early-activated splenic 6OXY-specific B cells correlated with vaccine efficacy

6OXY-KLH elicited GC and ASC B cells 14 days after immunization. Mice were immunized on days 0, 14 and 28, and challenged with 2.25 mg/kg oxycodone a week after the third immunization. Distribution of 6OXY-specific B cell subsets in spleen biopsies from individual mice: A) before, and B) after immunization. Immunization with 6OXY-KLH increased: C) the ratio of 6OXY-specific ($CD38^-$) to ($CD38^+$) $GL7^+$ B cells over time, and D) serum oxycodone concentrations. At 14 days post-vaccination: E) early GC activation, shown as the ratio of 6OXY-specific ($CD38^-$) to ($CD38^-$) $GL7^+$ B cells, and F) 6OXY-specific ASC B cells, correlated to greater vaccine efficacy on serum oxycodone at day 35. Data shown are the number of 6OXY-specific B cells per spleen biopsy sample from individual mice. Data are mean±SEM. Data included three independent experiments with a total n=12 each group. **p<0.01, and ***p<0.001 compared to KLH, ### p<0.001 compared to naïve mice; brackets indicate group differences.

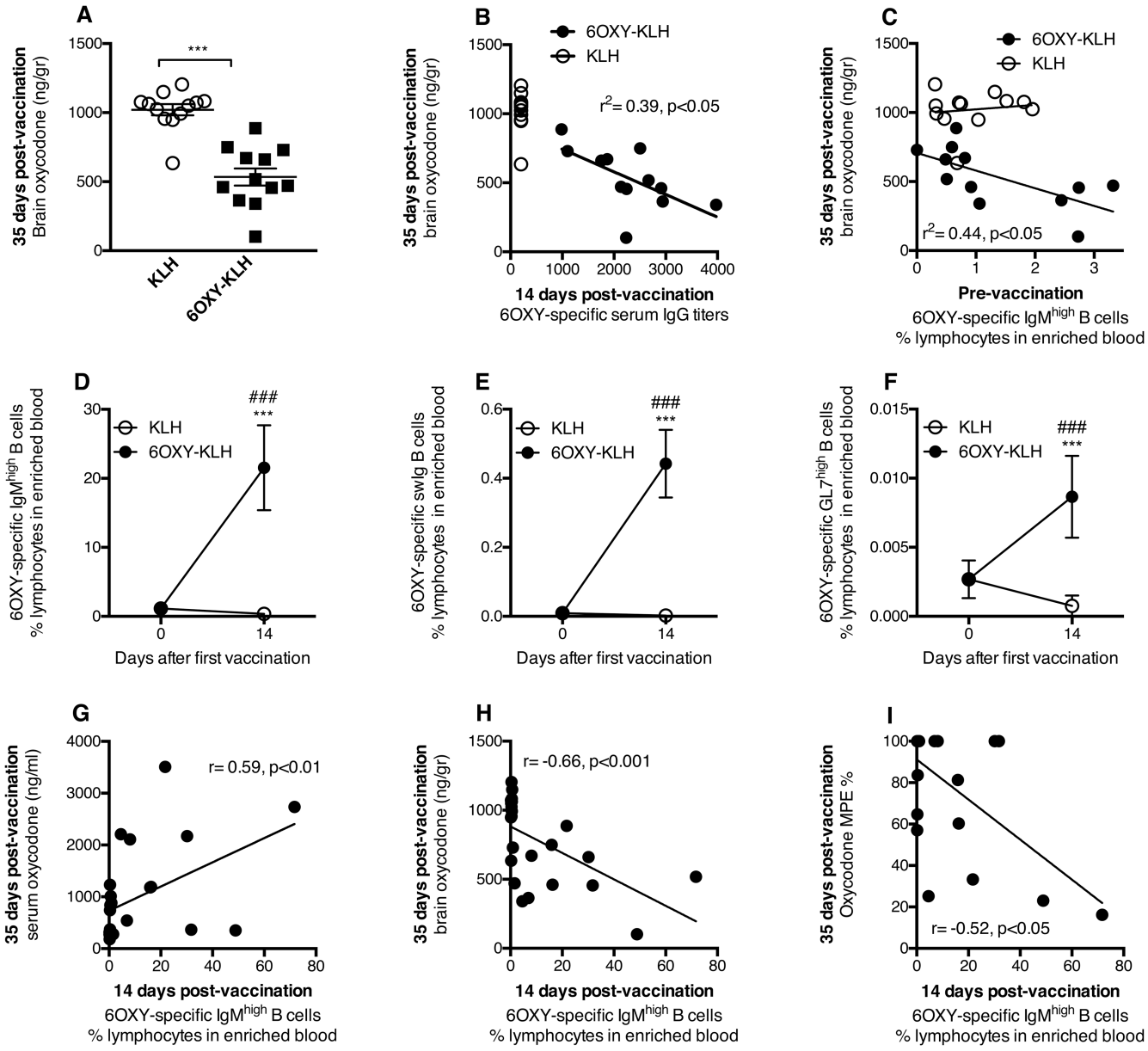

Figure 5. Frequency of hapten-specific B cells in blood correlates to vaccine efficacy

Using the $(6OXY)_4$-SA-PE and $(control)_4$-SA-PE-AF reagents and magnetic enrichment, B cells were analyzed in 200μl of blood collected before and after immunization with either 6OXY-KLH or KLH. A) Immunization reduced distribution of oxycodone to the brain, and B) early serum IgG titers correlated to subsequent blockage of oxycodone distribution to the brain. C) The frequency of 6OXY-specific IgM^{high} B cells prior to immunization correlated with vaccine efficacy in the 6OXY-KLH group. Immunization increased frequencies of 6OXY-specific B cell subsets D) IgM^{high}, E) swIg, and F) GC. Increased frequency of 6OXY-specific IgM^{high} B cells 14 days after the first immunization correlated to greater vaccine efficacy on oxycodone distribution to G) serum, H) brain, and I) oxycodone antinociception. Frequencies are the % of total lymphocytes in the bound fraction after

positive enrichment of blood. The MPE% represents hind paw flicks. Data are mean±SEM. Data include three independent experiment with a total n=12 each group. ### $p<0.001$ compared to naïve; ** $p<0.01$ compared to KLH control; *** $p<0.001$ compared to KLH control.

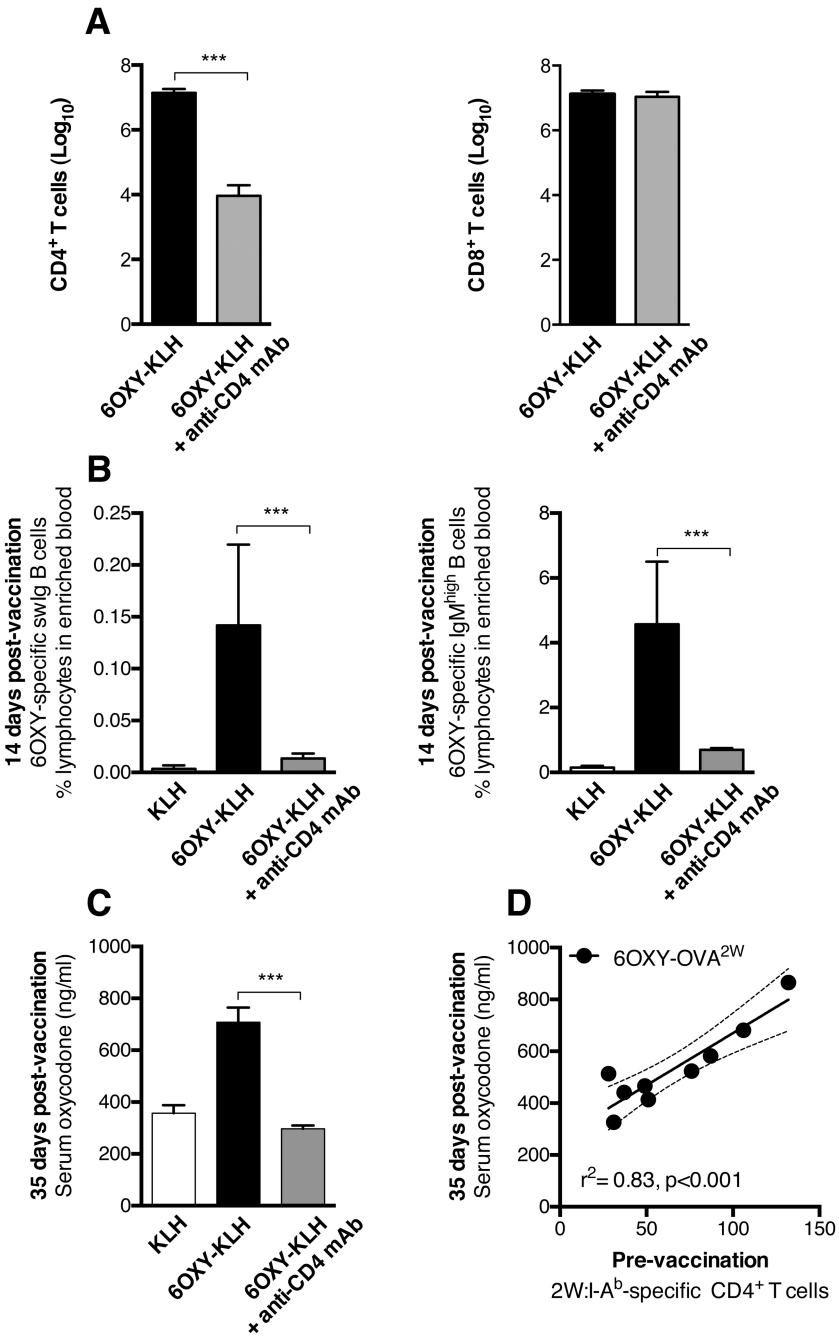

Figure 6. CD4$^+$ T cells-dependent B cell activation on vaccine efficacy

Selective depletion of CD4$^+$ T cells prevented activation of 6OXY-specific B cells and subsequent 6OXY-KLH effects in C57Bl/6 mice. A) Depletion of CD4$^+$ T cells, but not CD8$^+$ T cells in peripheral lymph nodes and spleen. T cells are shown as $\log_{10}$. B) The frequency of 6OXY-specific IgM^{high} and swIg B cells in enriched blood 14 days after the first immunization. C) Depletion of CD4$^+$ T cells blunted vaccine efficacy against oxycodone distribution measured on day 35, 7 days after the last immunization. D) In C57Bl/6 mice, an increased number of 2W1S-specific CD4$^+$ T cells in spleen biopsy prior to

immunization correlated to subsequent greater efficacy against oxycodone in mice vaccinated with 6OXY-OVA^{2W}. Data are mean±SEM. Data consists of two independent experiments for a total of (A-C) n=6 and (D) n=9 each group. *** $p<0.001$ compared to control or as indicated by brackets.

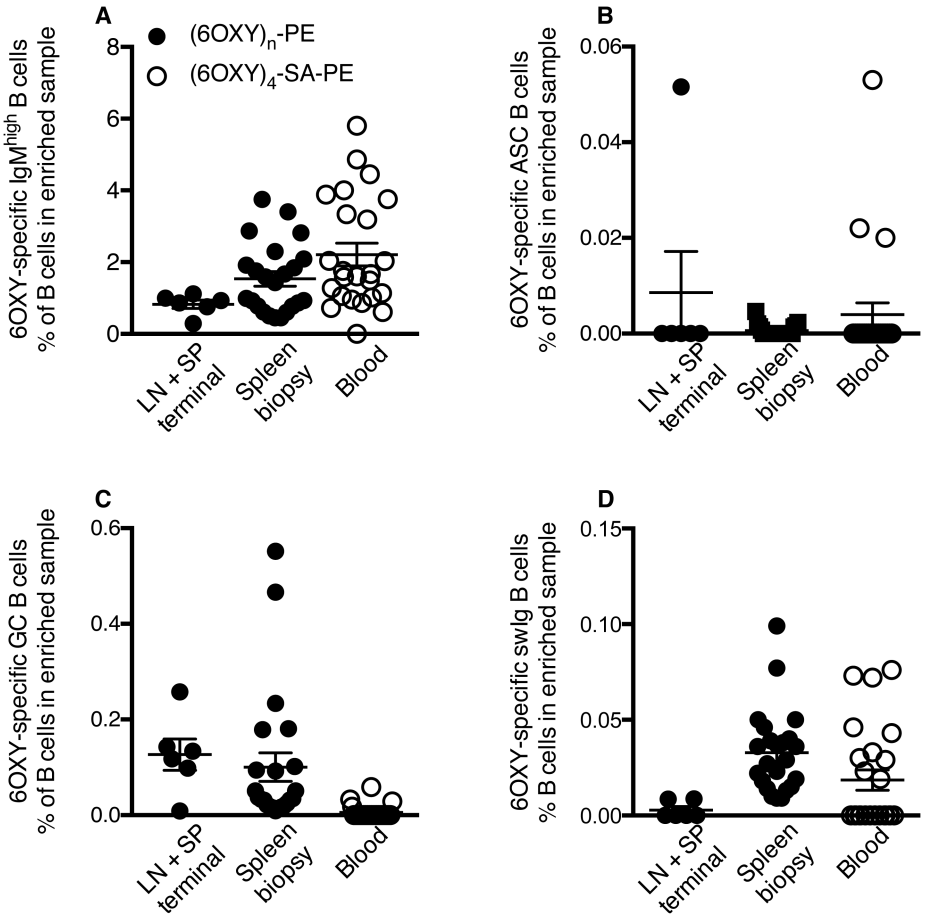

Figure 7. Frequency of hapten-specific B cells prior to immunization in mice

6OXY-specific naïve B cells (% of total B cells in enriched sample) in pooled mesenteric and peripheral lymph nodes and spleen (n= 6), spleen biopsy (n= 24) or blood (n=24) from naïve BALB/c mice. The frequency of 6OXY-specific B cells in lymph nodes and spleens (LN+LP) was calculated from a previously published study (23). B cell analysis in spleen biopsy and blood was performed in three independent experiments (8 mice each day). Mouse: A) 6OXY-specific IgM^{high} B cells, B) 6OXY-specific ASC B cells, C) 6OXY-specific GC B cells, and D) 6OXY-specific swIg B cells.